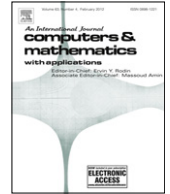




Contents lists available at SciVerse ScienceDirect

Computers and Mathematics with Applications

journal homepage: www.elsevier.com/locate/camwa

Synchronization and control of coupled reaction–diffusion systems of the FitzHugh–Nagumo type

B. Ambrosio*, M.A. Aziz-Alaoui

LMAH, FR-CNRS-3335, Université de Le Havre, ISCN, PRES Normandie Université, BP 540, 76058, Le Havre Cedex, France

ARTICLE INFO

Keywords:

Networks
Reaction–diffusion systems
Synchronization
Slow–fast systems
FitzHugh–Nagumo
Qualitative asymptotic behaviour

ABSTRACT

We consider a FitzHugh–Nagumo reaction–diffusion type system (FHN). The dynamics of the reaction part induces a unique repulsive stationary point $(0, 0)$ and a unique attractive limit cycle. After a description of the asymptotic behaviour of the FHN system, we deal with the synchronization and control analysis of N coupled FHN systems.

© 2012 Elsevier Ltd. All rights reserved.

1. Introduction

In 1952, after experiences on the squid giant axon, Hodgkin and Huxley proposed the first neuron model (see for example, [1–5]),

$$\begin{cases} C \frac{dV}{dt} = -\bar{g}_K n^4 (V - V_K) - \bar{g}_{Na} m^3 h (V - V_{Na}) - \bar{g}_L (V - V_L) + I \\ \frac{dm}{dt} = \alpha_m(V)(1 - m) - \beta_m(V)m \\ \frac{dn}{dt} = \alpha_n(V)(1 - n) - \beta_n(V)n \\ \frac{dh}{dt} = \alpha_h(V)(1 - h) - \beta_h(V)h \end{cases}$$

where,

V represents the membrane potential;

I represents an external applied current;

m , n and h , varying between 0 and 1, represent respectively the sodium activation, the sodium inactivation and the potassium activation. They determine the membrane permeability with respect to the associated ion;

C is the membrane capacitance;

\bar{g}_K , \bar{g}_{Na} and \bar{g}_L represent the maximal conductance of the membrane respectively for the potassium, sodium and leakage (mainly carried by chloride ions) current;

V_K , V_{Na} and V_L represent the Nernst equilibrium potential for potassium, sodium and leakage current. The α 's and β 's are functions of V , they represent the transfer rates, and have been experimentally determined by Hodgkin and Huxley. Thus, the Hodgkin–Huxley model gives a description of the main ionic fluxes across the neuron membrane creating the nervous signal. In 1961, FitzHugh proposed a 2D model that reproduces excitability and oscillatory features found in the

* Corresponding author.

E-mail address: benjamin.ambrosio@univ-lehavre.fr (B. Ambrosio).

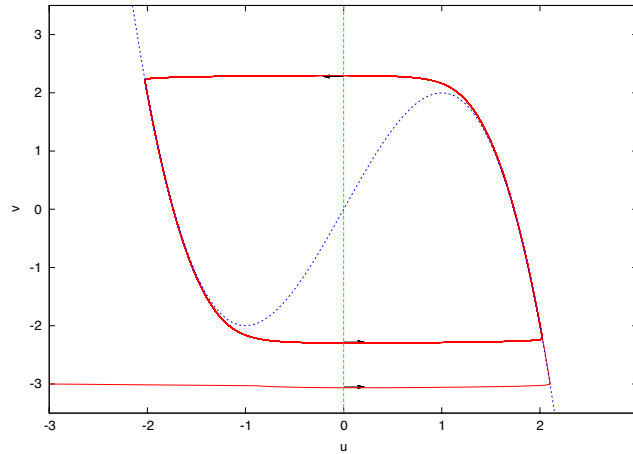


Fig. 1. Solutions of system (1).

Hodgkin–Huxley model; see [6]. It is a modification of the well-known Van der Pol model, and has been initially called, the Bonhoeffer–van der Pol (BVP) model,

$$\begin{cases} x_t = c(F(x) + y + z) \\ y_t = \frac{1}{c}(x - a + by) \end{cases}$$

with,

$$w_t = \frac{dw}{dt},$$

and where F is a cubic function, $a, b > 0$, z corresponds to a stimulus intensity.

In the same paper [6], FitzHugh showed that the quantities $u = V - 36m, w = 0.5(n - h)$ obtained from the Hodgkin–Huxley model evolve like the variables x and y of the BVP model. In 1962, Nagumo et al. proposed an electronic circuit whose behaviour is modelled by the BVP model; see [3]. The BVP model is now called the FitzHugh–Nagumo model. Another way to reduce the Hodgkin–Huxley to the FitzHugh–Nagumo model is to use properties of the Hodgkin–Huxley model and set, $h = 0.85 - n$ and $m(V) = \frac{\alpha_m(V)}{\alpha_m(V) + \beta_m(V)}$, then approximate the nullclines by a cubic and a straight line; see for example [2]. Thus, we consider here the following model of the FitzHugh–Nagumo type,

$$\begin{cases} \epsilon u_t = f(u) - v \\ v_t = u - \delta v \end{cases} \tag{1}$$

where

$$f(u) = -u^3 + 3u \quad \text{and} \quad \epsilon > 0, \delta > 0 \text{ are small parameters.}$$

In this case, all the solutions of system (1) different from $(0, 0)$ evolve towards the unique attractive limit cycle (see Fig. 1 and for example [7], in the limit case $\delta = 0$).

Based on model (1), we study a reaction–diffusion system of FitzHugh–Nagumo type (FHN) (see also [8]),

$$\begin{cases} \epsilon u_t = f(u) - v + d_u \Delta u \\ v_t = u - \delta v + d_v \Delta v \end{cases} \tag{2}$$

with $u = u(x, t), v = v(x, t)$, on a smooth bounded domain $\Omega \subset \mathbb{R}^n$ with $d_u, d_v > 0$ and with Neumann zero flux conditions on the boundary Γ of Ω ,

$$\frac{\partial u}{\partial \nu} = \frac{\partial v}{\partial \nu} = 0.$$

If the solutions of system (1) are well-known, what can we expect about the asymptotic behaviour of solutions of system (2)? This is the aim of the first part of Section 2, in which we also provide sufficient conditions under which the solutions go to $(0, 0)$. In the second part of this section, we extend the obtained result for N coupled systems of FHN type, $N = 1, 2, \dots$ and give results on synchronization phenomenon in the last section of this paper.

2. Analytical results on the space temporal behaviour of N coupled systems of FHN type

This section deals with the asymptotic behaviour of the solutions of N coupled systems of FHN type and mainly with the space homogeneous characteristic or pattern formation.

2.1. One system of FHN type

Our concern here, is the asymptotic behaviour of solutions of system (2) when those of system (1) are known. Such a question may be found, for example, in [9]. Using these techniques, one can prove the following result.

Theorem 1. *Let λ be the smallest non zero eigenvalue of the Laplacian operator with zero flux Neumann boundary conditions. If,*

$$3 - \lambda d_u < 0 \tag{3}$$

then,

$$\lim_{t \rightarrow +\infty} (\|u - \bar{u}\|_{L^2(\Omega)} + \|v - \bar{v}\|_{L^2(\Omega)}) = 0 \tag{4}$$

where,

$$\bar{u}(t) = \frac{\int_{\Omega} u(x, t) dx}{|\Omega|}, \quad \bar{v} = \frac{\int_{\Omega} v(x, t) dx}{|\Omega|}$$

and where \bar{u}, \bar{v} are solutions of the following system,

$$\begin{cases} \epsilon \bar{u}_t = f(\bar{u}) - \bar{v} + g(t) \\ \bar{v}_t = \bar{u} - \delta \bar{v} \end{cases} \tag{5}$$

with $g(t) \rightarrow 0$ with exponential rate when t goes to $+\infty$.

This means that, asymptotically, the solutions are space homogeneous, and for each $x \in \Omega$, solutions of system (2) are solutions of system (1) which,

- (i) either evolve around the limit cycle of (1),
- (ii) or evolve towards (0, 0).

Remark 1. Let us recall (see [9]) that the eigenvalue λ increases when the size of Ω decreases. This means that condition (3) is satisfied when the size of Ω is small or the diffusion coefficients d_u, d_v are large.

Proof of Theorem 1. Let $\phi(t) = \frac{1}{2}(\epsilon \|\nabla u\|_{L^2(\Omega)}^2 + \|\nabla v\|_{L^2(\Omega)}^2)$; then,

$$\begin{aligned} \dot{\phi} &= \int_{\Omega} (\epsilon \nabla u \nabla u_t + \nabla v \nabla v_t) \\ &= \int_{\Omega} (\nabla u \nabla (f(u) - v + d_u \Delta u) + \nabla v \nabla (u - \delta v + d_v \Delta v)) \\ &= \int_{\Omega} (f'(u) |\nabla u|^2 - \delta |\nabla v|^2 - d_u (\Delta u)^2 - d_v (\Delta v)^2) \\ &\leq \int_{\Omega} 3 |\nabla u|^2 - \lambda d_u \int_{\Omega} |\nabla u|^2 - \delta |\nabla v|^2 - \lambda d_v \int_{\Omega} |\nabla v|^2 \\ &\leq (3 - \lambda d_u) \int_{\Omega} |\nabla u|^2 - (\lambda d_v + \delta) \int_{\Omega} |\nabla v|^2. \end{aligned}$$

Now, since, $\lambda d_u > 3$ we have,

$$\dot{\phi} \leq -2 \min \left(\frac{\lambda d_u - 3}{\epsilon}, \lambda d_v + \delta \right) \phi$$

thus,

$$\phi(t) \leq \phi(0) e^{-c_1 t}$$

where,

$$c_1 = 2 \min \left(\frac{\lambda d_u - 3}{\epsilon}, \lambda d_v + \delta \right).$$

Furthermore,

$$\|u - \bar{u}\|_{L^2(\Omega)}^2 + \|v - \bar{v}\|_{L^2(\Omega)}^2 \leq \frac{1}{\lambda} (\|\nabla u\|_{(L^2(\Omega))^n}^2 + \|\nabla v\|^2 (L^2(\Omega))^n) \leq \frac{2}{\lambda \epsilon} \phi(t)$$

which implies (4). In the remaining of the proof, we show that, \bar{u} et \bar{v} are solutions of (5). We have,

$$\begin{cases} \epsilon \bar{u}_t = \frac{1}{|\Omega|} \int_{\Omega} f(u) - \bar{v} \\ \bar{v}_t = \bar{u} - \bar{v} \end{cases}$$

thus,

$$\begin{cases} \epsilon \bar{u}_t = \frac{1}{|\Omega|} \int_{\Omega} (f(u) - f(\bar{u})) + f(\bar{u}) - \bar{v} \\ \bar{v}_t = \bar{u} - \delta \bar{v} \end{cases}$$

that is,

$$\begin{cases} \epsilon \bar{u}_t = g(t) + f(\bar{u}) - \bar{v} \\ \bar{v}_t = \bar{u} - \delta \bar{v} \end{cases}$$

where,

$$g(t) = \frac{1}{|\Omega|} \int_{\Omega} (f(u) - f(\bar{u})).$$

But,

$$\begin{aligned} |g(t)| &= \left| \frac{1}{|\Omega|} \int_{\Omega} (f(u) - f(\bar{u})) \right| \\ &\leq \frac{M}{|\Omega|} \int_{\Omega} |u - \bar{u}| \\ &\leq \frac{M}{|\Omega|^{\frac{1}{2}}} \|u - \bar{u}\|_{L^2(\Omega)} \end{aligned}$$

where,

$$M = \sup_{t \in \mathbb{R}^+} |f'(\bar{u})|$$

since from a result in [7], we know that $(u, v) \in L^\infty(\Omega) \times L^\infty(\Omega)$, one can also see [10], which completes the proof. \square

The following proposition gives a sufficient condition to the occurrence of the asymptotic behaviour (ii) given by (6).

Proposition 1. *If condition (3) of Theorem 1 is satisfied and if,*

$$\int_{\Omega} u(x, 0) dx = \int_{\Omega} v(x, 0) dx = \int_{\Omega} f(u(x, 0)) dx = 0, \tag{7a}$$

and

$$\forall t \geq 0, \int_{\Omega} f(u(x, t)) dx = 0 \tag{7b}$$

then,

$$\lim_{t \rightarrow +\infty} (\|u\|_{L^2(\Omega)} + \|v\|_{L^2(\Omega)}) = 0.$$

Proof. By integrating system (2) and dividing by $|\Omega|$, we have,

$$\begin{cases} \epsilon \frac{\partial}{\partial t} \bar{u} = \frac{1}{|\Omega|} \int_{\Omega} f(u) - \bar{v} \\ \frac{\partial}{\partial t} \bar{v} = \bar{u} - \delta \bar{v} \end{cases} \tag{8}$$

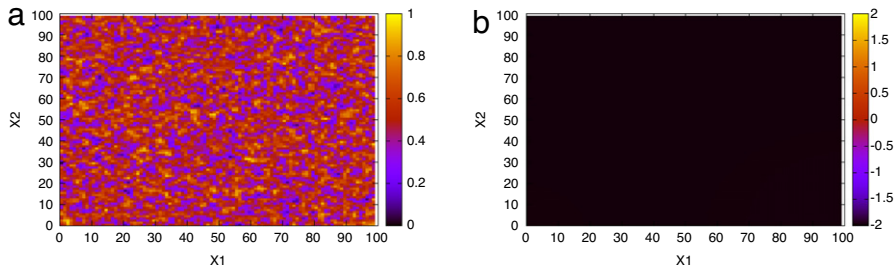


Fig. 2. Space homogeneous and periodic-time asymptotic behaviour of system (2) for almost initial conditions, with parameter values given by (9), (a) initial condition $u(x, 0)$, (b) asymptotic behaviour $u(x, 200)$.

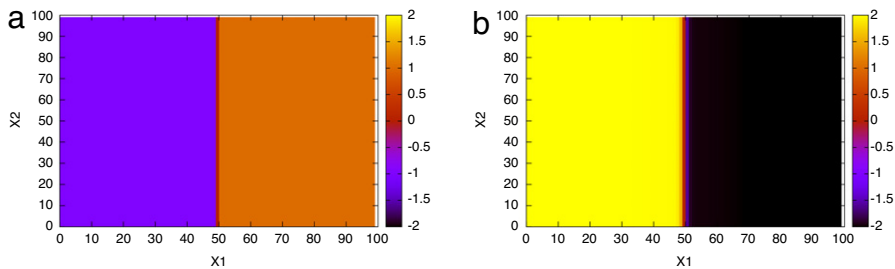


Fig. 3. Mirror asymptotic behaviour of system (2) for particular initial conditions near the set of functions satisfying (7a), with parameter values given by (9), (a) initial condition $u(x, 0)$, (b) asymptotic behaviour $u(x, 200)$.

since

$$\int_{\Omega} \Delta u dx = \int_{\Omega} \Delta v dx = 0,$$

and

$$(\bar{u}(t), \bar{v}(t)) = \left(\frac{\int_{\Omega} u(x, t) dx}{|\Omega|}, \frac{\int_{\Omega} v(x, t) dx}{|\Omega|} \right).$$

Thus, due to condition (7), we obtain, that $(0, 0)$ is the unique solution of Eq. (8).

Then, the result follows obviously from application of Theorem 1. \square

If condition (3) is satisfied, Theorem 1 gives a comprehensive description of the asymptotic behaviour. Either, the solutions of system (2) evolve towards solutions of kind (ii) given by (6), that is space homogeneous solution $(0, 0)$, and for this, (7) provides a sufficient condition, either solutions evolve toward solutions of kind (i) given by (6), that is the asymptotic behaviour is space homogeneous and time-periodic. Now, we consider the case where condition (3) is not satisfied and perform numerical simulations to analyse the asymptotic behaviour of solutions. We use the following parameter values,

$$\begin{cases} \Omega = [0, 100] \times [0, 100] \subset \mathbb{R}^2 \\ \epsilon = 0.1 \\ \delta = 0.001 \\ d_u = d_v = 1. \end{cases} \tag{9}$$

We observe that, if (7) is not satisfied, the system still evolves like solutions of kind (ii) given by (6). For instance, Fig. 2 shows such a behaviour in the case where the initial conditions $u(x, 0)$, $v(x, 0)$ follow a uniform law on the interval $[0, 1]$ for all $x = (x_1, x_2) \in \Omega$. This figure and all the following have been obtained, using an explicit finite difference scheme, with C++ language, and with a time step discretization equal to 0.01 and space step discretization equal to 1.

While, if condition (7) is satisfied, our numerical simulations show special patterns. Indeed, Fig. 3 shows a mirror solution of system (2) for particular initial conditions satisfying (7a). Likewise Figs. 4 and 5, show a spiral and a multiple spiral solutions of system (2) for particular initial conditions satisfying (7a).

Under the same conditions, as those used for Figs. 3–5, if we choose initial conditions following a uniform law on $[-1, 1]$ for all $x \in \Omega$, that is, near the set of functions satisfying condition (7a), our numerical simulations show a more complicated asymptotic behaviour as done in Fig. 6.

Remark 2. Let us remark that wave propagation and pattern formation are of great interest in understanding the behaviour of lot of systems and in particular the brain or cardiac dynamics. For example, in [11], and references therein cited, formation of spiral patterns have been experimentally shown in neocortex.

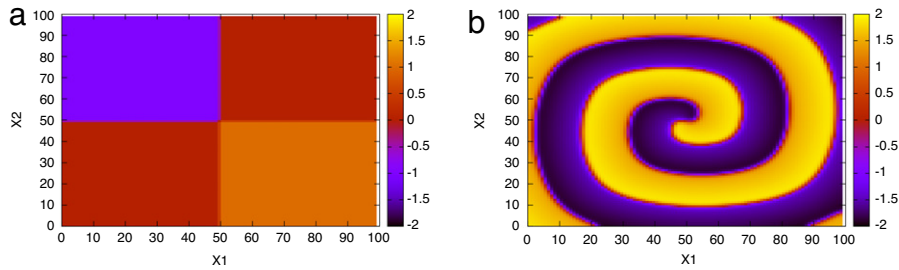


Fig. 4. Spiral asymptotic behaviour of system (2) for particular initial conditions near the set of functions satisfying (7a), with parameter values given by (9), (a) initial condition $u(x, 0)$, (b) asymptotic behaviour $u(x, 200)$.

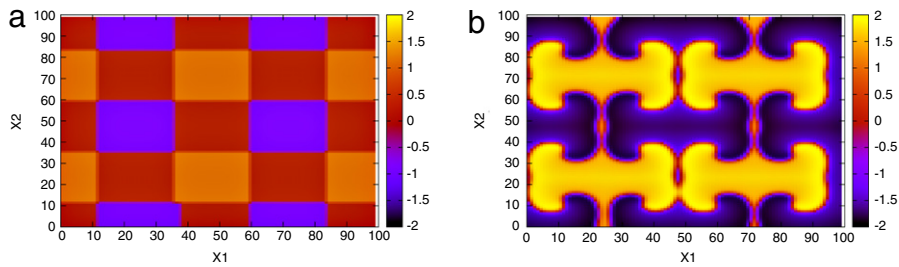


Fig. 5. Multiple spirals solution asymptotic behaviour of system (2) for particular initial conditions near the set of functions satisfying (7a), with parameter values given by (9), (a) initial condition $u(x, 0)$, (b) asymptotic behaviour $u(x, 200)$.

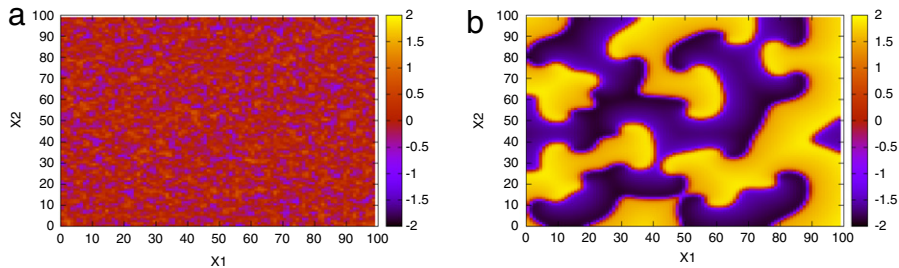


Fig. 6. Solution asymptotic behaviour of system (2) for particular random initial conditions near the set of functions satisfying (7a), with parameter values given by (9), (a) initial condition $u(x, 0)$, (b) asymptotic behaviour $u(x, 200)$.

2.2. Coupling N systems of FHN type

We can extend these results to N coupled systems of FHN type. Let us consider the following system,

$$\begin{cases} \epsilon u_{1t} = f(u_1) - v_1 + d_{u_1} \Delta u_1 \\ v_{1t} = u_1 - \delta_1 v_1 + d_{v_1} \Delta v_1 \\ \vdots \\ \epsilon u_{it} = f(u_i) - v_i + d_{u_i} \Delta u_i + \alpha_i (u_{i-1} - u_i) \\ v_{it} = u_i - \delta_i v_i + d_{v_i} \Delta v_i + \beta_i (v_{i-1} - v_i) \\ \vdots \\ \epsilon u_{Nt} = f(u_N) - v_N + d_{u_N} \Delta u_N + \alpha_N (u_{N-1} - u_N) \\ v_{Nt} = u_N - \delta_N v_N + d_{v_N} \Delta v_N + \beta_N (v_{N-1} - v_N) \end{cases} \quad (10)$$

where $\beta_i \geq 0$, for $i = 2, \dots, N$, and with zero flux boundary Neumann conditions. Then, if $\alpha_i = 0$, $i = 2, \dots, N$, we have the following result which can be also easily proved when $\alpha_i \neq 0$,

Theorem 2. Let λ be the smallest non zero eigenvalue of the Laplacian operator, with zero flux Neumann boundary conditions. Assume that,

$$3 - \lambda d_{u_i} < 0 \quad \forall i \in 1, \dots, N; \quad (11)$$

then,

$$\lim_{t \rightarrow +\infty} \sum_{i=1}^N (\|u_i - \bar{u}_i\|_{L^2(\Omega)} + \|v_i - \bar{v}_i\|_{L^2(\Omega)}) = 0, \tag{12}$$

where,

$$\bar{u}_i(t) = \frac{\int_{\Omega} u_i(x, t) dx}{|\Omega|}, \quad \bar{v}_i = \frac{\int_{\Omega} v_i(x, t) dx}{|\Omega|}, \quad \forall i \in 1, \dots, N$$

with (\bar{u}_i, \bar{v}_i) satisfying,

$$\begin{cases} \epsilon \bar{u}_{it} = f(\bar{u}_i) - \bar{v}_i + g_i(t) \\ \bar{v}_{it} = \bar{u}_i - \delta_i \bar{v}_i + \beta_i (\bar{v}_{i-1} - \bar{v}_i) \end{cases} \tag{13}$$

and where, $g_i(t) \rightarrow 0$ when $t \rightarrow +\infty$ with exponential rate decay.

Proof. It comes from an induction argument, by using similar techniques as those given in the proof of [Theorem 1](#). More precisely, let,

$$\phi_i = \frac{1}{2} \int_{\Omega} (\epsilon |\nabla u_i|^2 + |\nabla v_i|^2),$$

by algebraic computations we obtain,

$$\begin{aligned} \dot{\phi}_i &\leq (3 - \lambda d_{u_i}) \int_{\Omega} |\nabla u_i|^2 - \left(\lambda d_{v_i} + \delta_i + \frac{\beta_i}{2} \right) \int_{\Omega} |\nabla v_i|^2 + \frac{\beta_i}{2} \int_{\Omega} |\nabla v_{i-1}|^2 \\ &\leq (3 - \lambda d_{u_i}) \int_{\Omega} |\nabla u_i|^2 - \left(\lambda d_{v_i} + \delta_i + \frac{\beta_i}{2} \right) \int_{\Omega} |\nabla v_i|^2 + \frac{\beta_i}{2} K_{i-1} e^{-c_{i-1}t} \end{aligned}$$

where K_{i-1}, c_{i-1} are positive constants.

This yields,

$$\phi_i(t) \leq K_i e^{-c_i t}.$$

The remaining of the proof is similar as one of [Theorem 1](#). \square

Similarly, one can easily extend [Proposition 1](#).

Proposition 2. If condition (11) of [Theorem 2](#) are satisfied, and if,

$$\int_{\Omega} u_i(x, 0) dx = \int_{\Omega} v_i(x, 0) dx = 0,$$

and

$$\forall t \geq 0, \quad \int_{\Omega} f(u_i(x, t)) dx = 0$$

then,

$$\lim_{t \rightarrow +\infty} \sum_{i=1}^N (\|u_i\|_{L^2(\Omega)} + \|v_i\|_{L^2(\Omega)}) = 0. \tag{14}$$

Proof. Similar to the proof of [Proposition 1](#). \square

3. Synchronization

Synchronization phenomenon has been widely studied, mainly for ordinary or delay differential equations. However, for partial differential equations, only few results exist; see for example [[12–14](#)].

3.1. General result for coupled FHN systems

Definition 1. Let $S_i = (u_i, v_i)$. We say that S_i and S_j synchronize if,

$$\lim_{t \rightarrow +\infty} (\|u_i - u_j\|_{L^2(\Omega)} + \|v_i - v_j\|_{L^2(\Omega)}) = 0.$$

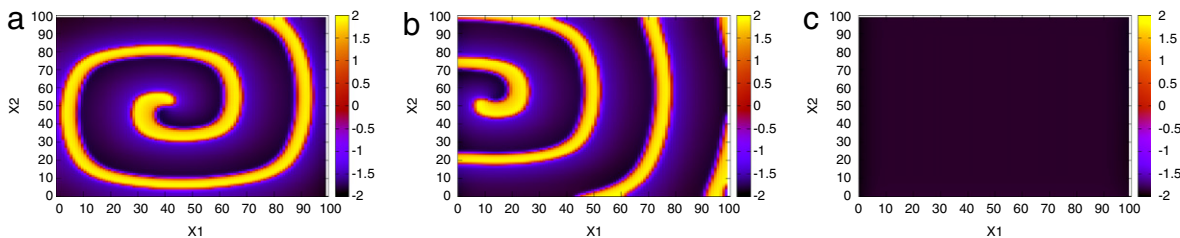


Fig. 7. Synchronization of two systems of type FHN for $\delta = 0.001$ and $\epsilon = 0.1$. Isovalues, of $u_2(x, t)$ at fixed time $t = 200$ and respectively for the coupling strength (a) $\beta_2 = 0.15$, (b) $\beta_2 = 0.15441558$ and (c) $\beta_2 = 0.15441559$.

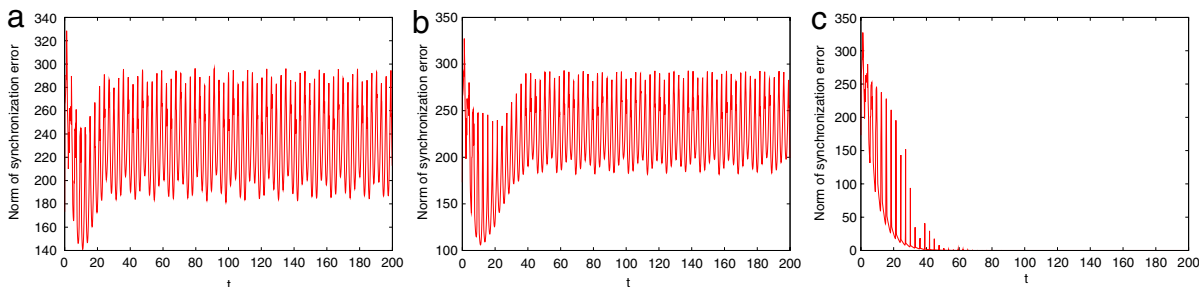


Fig. 8. Synchronization of two systems of type FHN for $\delta = 0.001$ and $\epsilon = 0.1$. The norm of synchronization error given by the Definition 1 on interval of time $[0, 200]$ for the coupling strength respectively (a) $\beta_2 = 0.15$, (b) $\beta_2 = 0.15441558$ and (c) $\beta_2 = 0.15441559$.

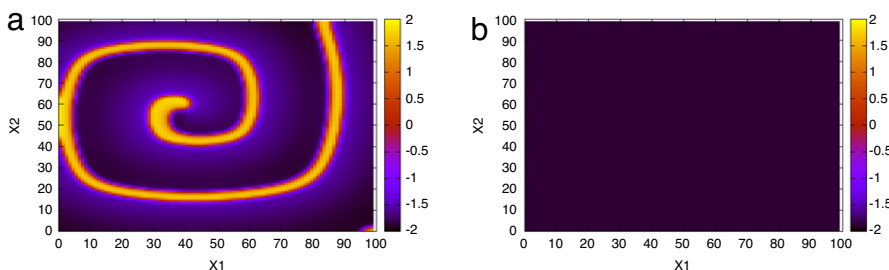


Fig. 9. Synchronization of three systems of type FHN for $\delta = 0.001$ and $\epsilon = 0.1$. Isovalues, of $u_3(x, t)$ at fixed time $t = 200$ and respectively for the coupling strength (a) $\beta_2 = \beta_3 = 0.23$, (b) $\beta_2 = \beta_3 = 0.24$.

Our numerical simulations (see Figs. 7 and 8) show that system (15) synchronize for a coupling strength β_2 belonging to the interval $[0.15441558, 0.15441559]$. In this figure, the initial conditions are $u_1(x, 0) = v_1(x, 0) = 1$ and $u_2(x, 0), v_2(x, 0)$ particular functions leading to the spiral pattern formation as done in Fig. 4.

Now, we consider three coupled FHN systems,

$$\begin{cases} \epsilon u_{1t} = f(u_1) - v_1 + \Delta u_1 \\ v_{1t} = u_1 - \delta v_1 + \Delta v_1 \\ \epsilon u_{2t} = f(u_2) - v_2 + \Delta u_2 \\ v_{2t} = u_2 - \delta v_2 + \Delta v_2 + \beta_2(v_1 - v_2) \\ \epsilon u_{3t} = f(u_3) - v_3 + \Delta u_3 \\ v_{3t} = u_3 - \delta v_3 + \Delta v_3 + \beta_3(v_2 - v_3). \end{cases} \quad (16)$$

Our numerical simulations (see Figs. 9 and 10) show that system (16) synchronize for a coupling strength $\beta_2 = \beta_3$ belonging to the interval $[0.23, 0.24]$. In this figure, the initial conditions are $u_1(x, 0) = v_1(x, 0) = 1$ and $(u_2(x, 0), v_2(x, 0)) = (u_3(x, 0), v_3(x, 0))$ particular functions leading to the spiral pattern formation as done in Fig. 4.

4. Conclusion

In this paper, we have studied a reaction–diffusion FitzHugh–Nagumo type system. A natural question was how the asymptotic behaviour of the PDE was related to one of the ODE. By using techniques from existing works we have comprehensively responded to this question in case where a condition on the Laplacian operator was satisfied. In particular,

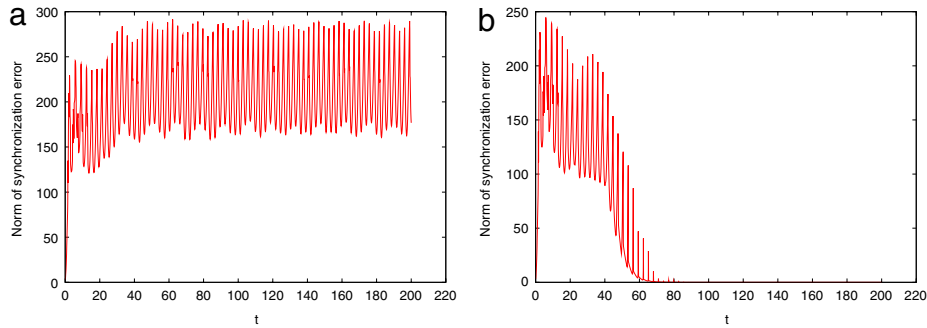


Fig. 10. Synchronization of three systems of type FHN for $\delta = 0.001$ and $\epsilon = 0.1$. The norm of synchronization error between S_2 and S_3 given by Definition 1 on the interval of time $[0, 200]$ for the coupling strength respectively (a) $\beta_2 = \beta_3 = 0.23$, (b) $\beta_2 = \beta_3 = 0.24$.

this condition is verified if the domain has a small size or if the diffusion coefficients are large. We also exhibited a condition that allows the formation of special spatial time-periodic patterns. These patterns have been observed in brain or cardiac dynamics. We then extended our results to N coupled FHN systems, and studied a synchronization phenomenon. In neuroscience context, this can be interpreted in terms of control. Particular neurons or external signals could be used to control the behaviour of other ones. Several open questions and further work on FHN systems are in progress and left to forthcoming papers.

Acknowledgements

This work was supported by Region Haute Normandie, France, and FEDER-RISC.

References

- [1] A.L. Hodgkin, A.F. Huxley, A quantitative description of membrane current and its application to conduction and excitation in nerve, *J. Physiol.* 117 (1952) 500–544.
- [2] E.M. Izhikevich, *Dynamical Systems in Neuroscience*, The MIT Press, 2007.
- [3] J. Nagumo, S. Arimoto, S. Yoshizawa, An active pulse transmission line simulating nerve axon, *Proc. IRE.* 50 (1962) 2061–2070.
- [4] J.P. Keener, J. Sneyd, *Mathematical Physiology I, Cellular Physiology*, Springer, 2009.
- [5] J.D. Murray, *Mathematical Biology*, Springer, 2010.
- [6] R.A. FitzHugh, Impulses and physiological states in theoretical models of nerve membrane, *Biophys. J.* 1 (1961) 445–466.
- [7] B. Ambrosio, Wave propagation in excitable media: numerical simulations and analytical study, in french. Ph.D. Thesis, Université Paris VI, 2009.
- [8] B. Ambrosio, J.-P. Françoise, Propagation of bursting oscillations, *Phil. Trans. R. Soc. A* 367 (2009) 4863–4875.
- [9] E. Conway, D. Hoff, J. Smoller, Large-time behaviour of solutions of systems of nonlinear reaction–diffusion equations, *SIAM J. Appl. Math.* 35 (1978) 1–16.
- [10] M. Marion, Finite-dimensionnal attractors associated with partly dissipative reaction–diffusion systems, *SIAM J. Math. Anal.* 20 (1989) 816–844.
- [11] Xiaoying Huang, Weifeng Xu, Jianmin Liang, Kentaroh Takagaki, Xin Gao, Jian young Wu, Spiral wave dynamics in neocortex, *Neuron* 68 (2010) 978–990.
- [12] P. Garcia, A. Acosta, H. Leiva, Synchronization conditions for master–slave reaction diffusion systems, *Europhysics Letters* 88 (2009) 60006.
- [13] L. Kocarev, Z. Tsarev, U. Parlitz, Synchronizing spatiotemporal chaos of partial differential equations, *Phys. Rev. Lett.* 79 (1997) 51–54.
- [14] Z. Xu, Synchronization of two discrete Ginzburg–Landau equations using local coupling, *Int. J. Nonlinear Sci.* 1 (2006) 19–29.